IJE TRANSACTIONS C: Aspects Vol. 31, No. 6, (June 2018) 986-996

International Journal of Engineering

Journal Homepage: www.ije.ir

# Study of Volumetric Flow Rate of a Micropump Using a Non-classical Elasticity Theory

A. M. Pasandi[a], S. Afrang[a], S. Dowlati[a], N. Sharafkhani[b], G. Rezazadeh[*c]

[a] *Electrical Engineering Department, Urmia University, Urmia, Iran*
[b] *Mechanical Engineering Department, Tabriz University, Tabriz, Iran*
[c] *Mechanical Engineering Department, Urmia University, Urmia, Iran*

*PAPER INFO*

*Paper history:*
Received 11 May 2016
Received in revised form 08 November 2017
Accepted 02 December 2017

*Keywords*:
Microelectromechanical Systems
Micropump
Pull-in Phenomenon
Couple Stress Theory

*ABSTRACT*

The purpose of this research is to study the mechanical behavior of a micropump with clamped circular diaphragm which is the main component of drug delivery systems. In this paper, the non-linear governing equations of the circular microplate using Kirchhoff thin plate theory was been extracted based on the modified couple stress (MCST) and classical (CT) theories. Then, the non-linear equation of static deflection is solved using Step-by-Step Linearization Method (SSLM) in order to escape the nonlinearity of the differential equation and Galerkin-based reduced-order model is applied to investigate the dynamic motion of the microplate. Afterwards, static and dynamic stabilities of the micropump have been studied based on both MCST and CT, then compared. Also, volumetric flow rate of the micropump was been delved based on both theories and in entire research, presence of the length scale parameter in modified couple stress theory brings this opportunity to study the size effect on the mechanical behavior of the micropump.

***doi**: 10.5829/ije.2018.31.06c.17*

## 1. INTRODUCTION

Microelectromechanical systems (MEMS) technology has been quickly growing since its arising in1980s as sensors and actuators. They provide light weight, small size and low-energy consumption [1]. It has been rapidly growing in order to provide fabrication of hundreds of accurate and miniaturized devices on a single wafer [2, 3]. The MEMS technology is an efficient technology in many related areas such as automobile [4] and aerospace [5] industries for instance in the smart mobile phones [6], biomedical [7] and so on. Therefore, MEMS can be considered as a dominant research field especially in biomedical applications.

Micropumps technology is one of the prominent technologies in MEMS in medical arena. The micropump is the main component of drug delivery systems that provides the actuation mechanism to deliver specific volumes of therapeutic agents/drugs from the reservoir [8]. Micropumps are classifiable into mechanical and non-mechanical ones. The micropumps which pump agents/drugs with the help of mechanical movements are referred as mechanical micropumps while in non-mechanical micropumps, there are no mechanical moving parts in order to pump. For activation of mechanical micropumps, a physical actuator is needed [9]. Electrostatic actuation is one of the actuation methods which is greatly considered owing to its simplicity, high-flow output pressure, fast response time and low power consumption [10]. Judy et al. [11] fabricated the first electrostatic micropump using surface micromachining technology. Zengerle et al. [12] presented a micropump with the flow rate of 70 μL/min at applied voltage of 170 V. Machauf et al. [13] reported the flow rate of 1 μL/min at applied voltage of 50 V. By using reduced order model of membrane, Liu [14] reported the "pull-in phenomena" in electrostatic micropump. Various parameters like radius, thickness, initial gap, residual stress on pull-in voltage and pull in position were delved [14]. A modeling of a micropump

*Corresponding Author's Email: g.rezazadeh@urmia.ac.ir (G. Rezazadeh)

Please cite this article as: A. M. Pasandi, S. Afrang, S. Dowlati, N. Sharafkhani, G. Rezazadeh, Study of Volumetric Flow Rate of a Micropump Using a Non-classical Elasticity Theory, International Journal of Engineering (IJE), IJE TRANSACTIONS C: Aspects Vol. 31, No. 6, (June 2018) 986-996

membrane with electrostatic actuator was developed by Lil et al. [15].

Micro scale devices deal with forces which are completely different from forces incorporating in the conventional scale devices. This is because the size of a physical system bears a significant effect on the physical phenomena determining the dynamic behavior of that system [16]. To design a precise and reliable micropump, studying of the mechanical behavior of the microplates is a crucial issue, including the static and dynamic instabilities or Pull-in phenomenon. Pull-in phenomenon is a discontinuity related to the interplay of the elastic and electrostatic forces. Applying a potential difference between a conducting structure and a ground level, the structure deforms due to electrostatic forces. By increasing the voltage the displacement reaches a point that no stable equilibrium exists and leading to the collapse and failure of the structure [17]. At pull-in point, the elastic restoring force can no longer resist the electrostatic force. The more increment of the voltage will cause the structure to have dramatic displacement jump [18]. Pull-in instability has been investigated by several researchers owing to its indispensable role in the design of MEMS structures [18-21].

Numerous experiments have been done in micro [16, 18] and nano-scale [22, 23] structures and it is perceived from hybrid atomistic-continuum model and experimental results [24, 25]. There is a size effect in micron and sub-micron scales which has a key role in the mechanical behavior of the microstructures [26]. It maintains that the classical theory of elasticity does not touch the accurate and definite characterizations of deformation occurrence due to not including the size effect. As a consequence, deficiencies in classical theory (CT) make them impossible to predict their behavior precisely. Recently, a number of non-classical theories such as strain gradient theories [27] nonlocal elasticity theory [28, 29] and couple stress theory [30] have been introduced and developed. The classical couple stress theory was originated by the Cosserat brothers [31], Toupin [30], Mindlin and Tiersten [32], to delve into the size-dependent effects on mechanical behavior of the microstructures. They utilized two length scale to capture the size effects. Due to difficulties in calculations of classical couple stress theory, Yang et al. [33] has developed modified couple stress theory (MCST) which provides a symmetric couple stress tensor and only a single internal length-scale parameter is involved instead of two classical lame's constants. For static analysing of isotropic micro-plates with arbitrary shapes based on the modified couple stress theory (MCST), Tsiatas attained a new Kirchhoff plate model. It contains only one material length scale parameter, which can capture the size effect [26]. Jomehzadeh et al. [34] presented the new model for vibration analysis of rectangular and circular micro-plates using a modified couple stress theory. Rashvand et al. [1] derived a Kirchhoff plate model for the dynamic analysis of a rectangular micro-plate using MCST considering stretching effect.

The majority of the investigations around the mechanical behavior of the micropumps are restricted to classical theories which have not been concerned with length scale parameter effect so they may lead to the inaccurate predictions. Accordingly, the necessities of studying the mechanical behavior of these devices by non-classical theories become a crucial issue.

This paper investigates the mechanical behavior of the micropump using higher order elasticity theories and delves into the size-dependent behavior of the circular microplate using the non-classical theory in comparison to the classical one. For this aim, the differential equations of a micropump are formulated by Kirchhoff thin plate theory applying MCST. Then, the non-linear equation of static deflection is solved using Step-by-Step Linearization Method (SSLM). In order to escape the nonlinearity of the differential equation and Galerkin-based reduced-order model is applied to investigate the dynamic motion of the microplate. Afterwards, the pull-in instability of the micropump subjected to an electrostatic force is studied based on the MCST for different length scale ratios and compared to results obtained by CT. In addition, volumetric flow rate of the micropump which is a function of the excitation frequency and amplitude is investigated using MCST for different length scale ratios.

## 2. MODEL DESCRIPTION AND MATHEMATICAL MODELLING

The mechanical micropumps have moving parts so a physical actuator for the pumping process is required. The most common mechanical micropumps are displacement-typed micropumps that involve a pumping chamber which is closed with a flexible diaphragm [8]. MEMS micropumps are generally modelled as two circular microplates as shown in Figure 1. The circular diaphragm undergoes more deflection in comparison to rectangular or square microplates. As a consequence, it has the most bending volume which makes it more appropriate for micropump. The isotropic thin movable upper plate with the thickness h, radius R, gap $g_0$ , density $\rho$, shear modulus G, Young's modulus E and Poisson's ratio $\nu$ is modelled using Kirchhoff plate theory. The lower plate must be thick enough, as it has no movement as the reference. The space between these plates is filled with a dielectric substance like air. By applying voltage the diaphragm vibrates.

An electrostatic force can be represented as follows:

$$F(w,V)=\frac{\varepsilon_0 V^2}{2(g_0-w(r,t))^2} \quad (1)$$

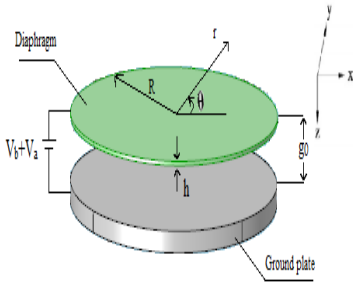


**Figure 1.** Schematic view of a circular electrostatically actuated micropump

where, $\varepsilon_0$ is the dielectric (permittivity) of the air, V is the applied voltage which consists of $V_b$ as the bias DC voltage and $V_a$ as the actuating voltage, $g_0$ is the initial gap between the diaphragm and the ground plate, t is the physical time and w(r,t) is the deflection of the diaphragm, defined to be positive downward. If $\frac{h}{2R}$ ratio is less than $\frac{1}{20}$, the plate can be assumed as a thin plate and the Kirchhoff thin plate theory can be utilized for studying mechanical behavior of the microplate[17].

The strain energy density, in an isotropic elastic material occupying a volume $V$ bounded by the surface $\Omega$ based on the modified couple stress theory introduced by Yang et al. [33] is given as follows:

$$\Pi=\frac{1}{2}\int_{V}\left(\sigma_{ij}:\varepsilon_{ij}+m_{ij}:\chi_{ij}\right)dV \tag{2}$$

In which $\sigma_{ij}$ is the Cauchy (classical) stress tensor, $\varepsilon_{ij}$ is strain tensor, $m_{ij}$ is the deviatoric part of the symmetric couple stress tensor and $\chi_{ij}$ is the symmetric part of the curvature tensor. It should be noted that in the classical theory, the strain energy density is the dot product of the stress and strain tensors. However, in the case of the modified couple stress theory the dot product of the deviatoric part of the symmetric couple stress and the symmetric part of the curvature tensors are added into the classical formulation and all are expressed as follows:

$$\sigma_{ij}=\lambda\varepsilon_{kk}\delta_{ij}+2\mu\varepsilon_{ij} \tag{3}$$

$$\varepsilon_{ij}=\frac{1}{2}(u_{i,j}+u_{j,i}) \tag{4}$$

$$m_{ij}=2\mu\ell^2\chi_{ij} \tag{5}$$

$$\chi_{ij}=\frac{1}{2}(\theta_{i,j}+\theta_{j,i}) \tag{6}$$

$$\theta_i=\frac{1}{2}e_{ijk}u_{k,j} \tag{7}$$

$$\lambda=\frac{E}{(1+\nu)(1-2\nu)} \quad \text{and} \quad \mu=\frac{E}{2(1+\nu)} \tag{8}$$

where, $u_i$ is the displacement vector, λ and μ are Lamé's constants, $\delta_{ij}$ is the Kronecker delta, $\ell$ is a material length-scale parameter, $\theta_i$ is the rotation vector and $e_{ijk}$ is the permutation symbol [33].

Based on Kirchhoff thin plate theory, the displacement components along the radial $u_r$, circumferential $u_\theta$ and axial $u_z$ directions have the relationship as follows:

$$u_r(r,\theta,z,t)=-z\frac{\partial w(r,\theta,t)}{\partial r} \tag{9}$$

$$u_\theta(r,\theta,z,t)=-z\frac{\partial w(r,\theta,t)}{r\partial\theta} \tag{10}$$

$$u_z(r,\theta,z,t)=w(r,\theta,t) \tag{11}$$

According to Equations (8), (9) and (10), in the cylindrical coordinate system the strain tensor can be expressed as:

$$\varepsilon=\begin{bmatrix}\frac{\partial u_r}{\partial r} & \frac{1}{2}\left(\frac{\partial u_r}{r\partial\theta}+\frac{\partial u_\theta}{\partial r}-\frac{u_\theta}{r}\right) & 0\\ \frac{1}{2}\left(\frac{\partial u_r}{r\partial\theta}+\frac{\partial u_\theta}{\partial r}-\frac{u_\theta}{r}\right) & \frac{u_r}{r}+\frac{\partial u_\theta}{r\partial\theta} & 0\\ 0 & 0 & 0\end{bmatrix}$$
$$=\begin{bmatrix}-z\frac{\partial^2 w}{\partial r^2} & -z\frac{\partial}{\partial r}\left(\frac{\partial w}{r\partial\theta}\right) & 0\\ -z\frac{\partial}{\partial r}\left(\frac{\partial w}{r\partial\theta}\right) & -z\left(\frac{\partial w}{r\partial\theta}+\frac{\partial^2 w}{r^2\partial\theta^2}\right) & 0\\ 0 & 0 & 0\end{bmatrix} \tag{12}$$

And curvature tensor can be written as:

$$\chi=\begin{bmatrix}\frac{\partial}{\partial r}\left(\frac{\partial w}{r\partial\theta}\right) & -\frac{1}{r}\frac{\partial w}{\partial r}+\frac{\partial^2 w}{r^2\partial\theta^2}-\frac{\partial^2 w}{\partial r^2} & 0\\ -\frac{1}{r}\frac{\partial w}{\partial r}+\frac{\partial^2 w}{r^2\partial\theta^2}-\frac{\partial^2 w}{\partial r^2} & -\frac{1}{r}\frac{\partial}{\partial\theta}\left(\frac{\partial w}{\partial r}\right) & 0\\ 0 & 0 & 0\end{bmatrix}$$
$$=\begin{bmatrix}-\frac{1}{r^2}\frac{\partial w}{\partial\theta}+\frac{1}{r}\frac{\partial^2 w}{\partial r\partial\theta} & -\frac{1}{r}\frac{\partial w}{\partial r}+\frac{\partial^2 w}{r^2\partial\theta^2}-\frac{\partial^2 w}{\partial r^2} & 0\\ -\frac{1}{r}\frac{\partial w}{\partial r}+\frac{\partial^2 w}{r^2\partial\theta^2}-\frac{\partial^2 w}{\partial r^2} & -\frac{1}{r}\frac{\partial^2 w}{\partial r\partial\theta} & 0\\ 0 & 0 & 0\end{bmatrix} \tag{13}$$

By using and replacing Equations (3) and (8) in one another, the stress tensor can be described as:

$$\sigma=\begin{bmatrix}\frac{E}{1-\nu^2}(\varepsilon_{rr}+\nu\varepsilon_{\theta\theta}) & G\gamma_{r\theta} & 0\\ G\gamma_{r\theta} & \frac{E}{1-\nu^2}(\varepsilon_{\theta\theta}+\nu\varepsilon_{rr}) & 0\\ 0 & 0 & 0\end{bmatrix}=$$

$$\begin{bmatrix}-\frac{E}{1-\nu^2}\left[\begin{matrix}z\frac{\partial^2 w}{\partial r^2}+\\ \nu z\left(\frac{1}{r}\frac{\partial w}{\partial r}+\\ \frac{1}{r^2}\frac{\partial^2 w}{\partial\theta^2}\right)\end{matrix}\right] & -2Gz\frac{\partial}{\partial r}\left(\frac{\partial w}{r\partial\theta}\right) & 0\\ -2Gz\frac{\partial}{\partial r}\left(\frac{\partial w}{r\partial\theta}\right) & -\frac{E}{1-\nu^2}\left[z\left(\begin{matrix}\frac{1}{r}\frac{\partial w}{\partial r}+\\ \frac{1}{r^2}\frac{\partial^2 w}{\partial\theta^2}\end{matrix}\right)+\nu z\frac{\partial^2 w}{\partial r^2}\right] & 0\\ 0 & 0 & 0\end{bmatrix} \quad (14)$$

Similarly, the couple stress tensor can be obtained as:

$$m=\begin{bmatrix}2G\ell^2\frac{\partial}{\partial r}\left(\frac{1}{r}\frac{\partial w}{\partial\theta}\right) & -2G\ell^2\left(\begin{matrix}\frac{1}{r}\frac{\partial w}{\partial r}-\frac{1}{r^2}\frac{\partial^2 w}{\partial\theta^2}\\ +\frac{\partial^2 w}{\partial r^2}\end{matrix}\right) & 0\\ -2G\ell^2\left(\begin{matrix}\frac{1}{r}\frac{\partial w}{\partial r}-\frac{1}{r^2}\frac{\partial^2 w}{\partial\theta^2}\\ +\frac{\partial^2 w}{\partial r^2}\end{matrix}\right) & -2G\ell^2\frac{1}{r}\frac{\partial}{\partial\theta}\left(\frac{\partial w}{\partial r}\right) & 0\\ 0 & 0 & 0\end{bmatrix} \quad (15)$$

where, G=E/2(1+ν) is the shear modulus.

According to the Equations (14) and (15) the bending moments by the classic stress tensor [35] and the couple stress tensor respectively, can be achieved as follows:

$$M^{\sigma}=\int_{-h/2}^{+h/2} z\begin{bmatrix}\sigma_{rr} & \tau_{r\theta} & 0\\ \tau_{r\theta} & \sigma_{\theta\theta} & 0\\ 0 & 0 & 0\end{bmatrix}dz=$$

$$\begin{bmatrix}-D\left[\begin{matrix}\frac{\partial^2 w}{\partial r^2}+\nu\left(\begin{matrix}\frac{1}{r}\frac{\partial w}{\partial r}+\\ \frac{1}{r^2}\frac{\partial^2 w}{\partial r^2}\end{matrix}\right)\end{matrix}\right] & -D(1-\nu)\frac{\partial}{\partial r}\left(\frac{1}{r}\frac{\partial w}{\partial\theta}\right) & 0\\ -D(1-\nu)\frac{\partial}{\partial r}\left(\frac{1}{r}\frac{\partial w}{\partial\theta}\right) & -D\left[\left(\begin{matrix}\frac{1}{r}\frac{\partial w}{\partial r}+\\ \frac{1}{r^2}\frac{\partial^2 w}{\partial\theta^2}\end{matrix}\right)+\nu\frac{\partial^2 w}{\partial r^2}\right] & 0\\ 0 & 0 & 0\end{bmatrix} \quad (16)$$

$$M^{m}=\int_{-h/2}^{+h/2} z\begin{bmatrix}m_{rr} & m_{r\theta} & 0\\ m_{r\theta} & m_{\theta\theta} & 0\\ 0 & 0 & 0\end{bmatrix}dz=$$

$$\begin{bmatrix}2D^{\ell}\frac{\partial}{\partial r}\left(\frac{1}{r}\frac{\partial w}{\partial\theta}\right) & -2D^{\ell}\left(\begin{matrix}\frac{1}{r}\frac{\partial w}{\partial r}-\frac{1}{r^2}\frac{\partial^2 w}{\partial\theta^2}+\\ \frac{\partial^2 w}{\partial r^2}\end{matrix}\right) & 0\\ -2D^{\ell}\left(\begin{matrix}\frac{1}{r}\frac{\partial w}{\partial r}-\frac{1}{r^2}\frac{\partial^2 w}{\partial\theta^2}\\ +\frac{\partial^2 w}{\partial r^2}\end{matrix}\right) & -2D^{\ell}\frac{1}{r}\frac{\partial}{\partial\theta}\left(\frac{\partial w}{\partial r}\right) & 0\\ 0 & 0 & 0\end{bmatrix} \quad (17)$$

where, D is the classical bending rigidity of the plate and $D^{\ell}$ is the contribution of rotation gradients to the bending rigidity and respectively are given as:

$$D=\frac{Eh^3}{12(1-\nu^2)} \quad , \quad D^{\ell}=G\ell^2 h=\frac{E\ell^2 h}{2(1+\nu)} \quad (18)$$

Hamilton principle certifies, the actual motion minimizes the difference of the kinetic energy and total potential energy for a system with prescribed configurations at t =[0,T] [36] as follows:

$$\delta\int_0^T\left[K-(\Pi-W)\right]dt=0 \quad (19)$$

In which K is kinetic energy $\Pi$ is the strain energy and W is the work of external loads of the microplate. The kinetic energy of the circular diaphragm is given by:

$$K=\frac{1}{2}\int_{V}\rho\left[\left(\frac{\partial u_r}{\partial t}\right)^2+\left(\frac{\partial u_\theta}{\partial t}\right)^2+\left(\frac{\partial u_z}{\partial t}\right)^2\right]dV \quad (20)$$

where, ρ is the mass density of material. Considering $\frac{\partial u_r}{\partial t}=\frac{\partial u_\theta}{\partial t}=0$, the first variations of total kinetic energy of the diaphragm on the time interval [0, T] can be expressed as:

$$\delta\int_0^T K dt=-\int_0^T\int_\Gamma\rho h\left(\frac{\partial w}{\partial t}\right)^2\delta w\, d\Gamma dt \quad (21)$$

The work done by the external forces in the form of transverse loading $q(r,\theta)$ and as a consequence, the first variations of the work on the time interval [0, T] can be achieved respectively as:

$$W^{ext}=\int_\Gamma q(r,\theta)w(r,\theta)\, d\Gamma \quad (22)$$

$$\delta\int_0^T W dt=\int_0^T\int_\Gamma q(r,\theta)\delta w\ d\Gamma dt \quad (23)$$

By using and replacing Equations (2), (16) and (17) the strain energy density can be written as:

$$\Pi = \frac{1}{2}\int_{\Gamma}\{-M_{rr}^{\sigma}\frac{\partial^2 w}{\partial r^2} - M_{\theta\theta}^{\sigma}\left(\frac{1}{r}\frac{\partial w}{\partial r}+\frac{1}{r^2}\frac{\partial^2 w}{\partial \theta^2}\right) -2M_{r\theta}^{\sigma}\frac{\partial}{\partial r}\left(\frac{1}{r}\frac{\partial w}{\partial \theta}\right)+M_{rr}^{m}\frac{\partial}{\partial r}\left(\frac{1}{r}\frac{\partial w}{\partial \theta}\right)-M_{\theta\theta}^{m} \frac{\partial}{\partial \theta}\left(\frac{1}{r}\frac{\partial w}{\partial r}\right)-M_{r\theta}^{m}\left(\frac{1}{r}\frac{\partial w}{\partial r}-\frac{1}{r^2}\frac{\partial^2 w}{\partial \theta^2}+\frac{\partial^2 w}{\partial r^2}\right)\}d\Gamma \quad (24)$$

The first variation of the strain energy on the time interval [0,T] can be obtained as:

$$\delta\int_0^T \Pi dt = \int_0^T\int_{\Gamma}\{-\frac{\partial^2 M_{rr}^{\sigma}}{\partial r^2}-\frac{2}{r}\frac{\partial M_{rr}^{\sigma}}{\partial r}-\frac{1}{r^2}\frac{\partial^2 M_{\theta\theta}^{\sigma}}{\partial \theta^2}+\frac{1}{r}\frac{\partial M_{\theta\theta}^{\sigma}}{\partial r}-\frac{2}{r}\frac{\partial^2 M_{r\theta}^{\sigma}}{\partial r\partial\theta}-\frac{2}{r^2}\frac{\partial M_{r\theta}^{\sigma}}{\partial\theta}+\frac{1}{r}\frac{\partial^2 M_{rr}^{m}}{\partial r\partial\theta}+\frac{1}{r^2}\frac{\partial M_{rr}^{m}}{\partial\theta}-\frac{1}{r}\frac{\partial^2 M_{\theta\theta}^{m}}{\partial r\partial\theta}+\frac{1}{r}\frac{\partial M_{r\theta}^{m}}{\partial r}-\frac{2}{r}\frac{\partial M_{r\theta}^{m}}{\partial r}+\frac{1}{r^2}\frac{\partial^2 M_{r\theta}^{m}}{\partial\theta^2}-\frac{\partial^2 M_{r\theta}^{m}}{\partial r^2}\}\delta w d\Gamma dt \quad (25)$$

By substituting Equations (21), (23) and (25) into Equation (19), the governing equilibrium differential equation of the transverse motion for a circular microplate takes the form as:

$$\frac{\partial^2 M_{rr}^{\sigma}}{\partial r^2}+\frac{2}{r}\frac{\partial M_{rr}^{\sigma}}{\partial r}+\frac{1}{r^2}\frac{\partial^2 M_{\theta\theta}^{\sigma}}{\partial\theta^2}-\frac{1}{r}\frac{\partial M_{\theta\theta}^{\sigma}}{\partial r}+\frac{2}{r}\frac{\partial^2 M_{r\theta}^{\sigma}}{\partial r\partial\theta}+\frac{2}{r^2}\frac{\partial M_{r\theta}^{\sigma}}{\partial\theta}-\frac{1}{r}\frac{\partial^2 M_{rr}^{m}}{\partial r\partial\theta}-\frac{1}{r^2}\frac{\partial M_{rr}^{m}}{\partial\theta}+\frac{1}{r}\frac{\partial^2 M_{\theta\theta}^{m}}{\partial r\partial\theta}-\frac{1}{r}\frac{\partial M_{r\theta}^{m}}{\partial r}+\frac{2}{r}\frac{\partial M_{r\theta}^{m}}{\partial r}-\frac{1}{r^2}\frac{\partial^2 M_{r\theta}^{m}}{\partial\theta^2}+\frac{\partial^2 M_{r\theta}^{m}}{\partial r^2}+q=\rho h\frac{\partial^2 w}{\partial t^2} \quad (26)$$

Replacement of Equations (16) and (17) into (26) results the governing equation of the micro-plate in terms of the deflection is as follows:

$$(D+D^{\ell})\nabla^4 w+\rho h\frac{\partial^2 w}{\partial t^2}=q \quad (27)$$

Dependency of the deflection only on the radial position r, originates from considering that the deflection of the plate is symmetrical relative to circumferential coordinate $\frac{\partial w}{\partial\theta}=0$. Consequently, the biharmonic operator, $\nabla^4$ in polar coordinate system for the axisymmetric circular microplate is expressed as:

$$\nabla^4=\nabla^2\nabla^2=\frac{\partial^4}{\partial r^4}+\frac{2}{r}\frac{\partial^3}{\partial r^3}-\frac{1}{r^2}\frac{\partial^2}{\partial r^2}+\frac{1}{r^3}\frac{\partial}{\partial r} \quad (28)$$

Note that is $\nabla^2$ the Laplace operator:

$$\nabla^2=\frac{\partial^2}{\partial r^2}+\frac{1}{r}\frac{\partial}{\partial r} \quad (29)$$

The clamped micropump's boundary conditions are given by:

$$\frac{\partial w}{\partial r}(R,t)=0 \quad , \text{w(R,t)=0} \quad (30)$$

Hence, the governing equation of the transverse motion for a circular microplate subjected to nonlinear electrostatic force can be written as:

$$(D+D^{\ell})\nabla^4 w+\rho h\frac{\partial^2 w}{\partial t^2}+C\frac{\partial w}{\partial t}=\frac{\varepsilon_0 V^2}{2(g_0-w)^2} \quad (31)$$

It should be noted that C is the equivalent damping of the system which includes fluid damping, thermoelastic damping and other internal dampings.

For convenience, the following non-dimensional parameters are defined in order to transformation of Equation (31) into non-dimensional form:

$$\hat{w}=\frac{w}{g_0},\hat{r}=\frac{r}{R},\hat{V}=\frac{V}{V^*},\hat{t}=\frac{t}{t^*},\hat{\omega}=\frac{\omega}{\omega^*},\quad t^*=R^2\sqrt{\frac{\rho h}{D}},V^*=\frac{1}{R^2}\sqrt{\frac{Dg_0^3}{\varepsilon_0}},\omega^*=\frac{1}{t^*} \quad (32)$$

Substituting Equation (32) into (31):

$$(\frac{D+D^{\ell}}{D})\nabla^4\hat{w}+\frac{\partial^2\hat{w}}{\partial\hat{t}^2}+\beta\frac{\partial\hat{w}}{\partial\hat{t}}=\frac{\hat{V}^2}{2(1-\hat{w})^2} \quad (33)$$

In which:

$$\beta=\frac{CR^4}{Dt^*} \quad (34)$$

## 3. NUMERICAL SOLUTIONS

**3. 1. Static Analysis** The equation of the static deflection of the circular diaphragm under bias DC voltage is solved using step-by-step linearization method (SSLM) due to the non-linearity of the equation and complexity and time consumption of the solution [3].

$$(\frac{D+D^{\ell}}{D})\nabla^4\hat{w}_s^{\,i}=\frac{\hat{V}^{i\,2}}{2(1-\hat{w}_s^{\,i})^2} \quad (35)$$

The SSLM is applied considering $\hat{w_s}^{i}$ as the diaphragm deflection due to the bias DC voltage $\hat{V}^{i}$ which is applied in the (i)th step. The amount of voltage rise in each step is $\delta\hat{V}$ to a new value $\hat{V}^{i+1}$ and as a result of that the deflection will be changed to $\hat{w_s}^{i+1}$:

$$\hat{V}^{i+1}\rightarrow\hat{V}^{i}+\delta\hat{V} \qquad and \qquad \hat{w}^{i+1}\rightarrow\hat{w}^{i}+\psi(\hat{r}) \quad (36)$$

Therefore, Equation (35) for the (i+1)th step can be written as follows:

$$(\frac{D+D^{\ell}}{D})\nabla^4 \hat{w}_s^{\,i+1} = \frac{\hat{V}^{\,i+1^2}}{2(1-\hat{w}_s^{\,i+1})^2} \quad (37)$$

To approach a desired accuracy, the small value of $\delta\hat{V}$ is assumed. Using the calculus of variation theory and Taylor expansion considering first two terms and neglecting the higher order terms of the series, the following linearized equation in order to calculate $\psi$ can be obtained:

$$(\frac{D+D^{\ell}}{D})\nabla^4 \psi(\hat{r}) - \frac{\hat{V}^{\,i^2}}{(1-\hat{w}_s^{\,i})^3}\psi(\hat{r}) = \frac{\hat{V}^{\,i^2}}{2(1-\hat{w}_s^{\,i})^2}\delta\hat{V} \quad (38)$$

$\psi(\hat{r})$ can be approximated the function space in terms of basis function as follows:

$$\psi_n(\hat{r}) = \sum_{n=1}^{N} a_n \varphi_n(\hat{r}) \quad (39)$$

where, $\varphi_n(\hat{r})$ are the shape functions satisfying the boundary conditions and $a_n$ are the unknown coefficients evaluated by using Galerkin weighed residual method in each step.

By substituting Equation (39) into Equation (38) and multiplying by the weight function $\varphi_i(\hat{r})$ in Galerkin-based weighed residual method and integrating the result with respect to r over [0, 1], a set of algebraic equations will be obtained as follows which leads to determine $a_n$:

$$\sum_{n=1}^{N}(K_{in})a_n = F_i \qquad \text{i=1,...,N} \quad (40)$$

where:

$$K_{in} = \int_0^1 \left( (\frac{D+D^{\ell}}{D})\nabla^4 \varphi_n(\hat{r})\varphi_i(\hat{r}) - \frac{\hat{V}^{\,2}}{(1-\hat{w}_s)^3}\varphi_n(\hat{r})\varphi_i(\hat{r}) \right) d\hat{r} \quad (41)$$

In which, $K_{in}$ is including $K^{mech}$ and $K^{elec}$ which are mechanical and electrical stiffness, respectively as follows and applying voltage reduces mechanical stiffness of the system.

$$K_{in}^{mech} = \int_0^1 \left( (\frac{D+D^{\ell}}{D})\nabla^4 \varphi_n(\hat{r})\varphi_i(\hat{r}) \right) d\hat{r} \quad (42)$$

$$K_{in}^{elec} = \int_0^1 \left( \frac{\hat{V}^{\,2}}{(1-\hat{w}_s)^3}\varphi_n(\hat{r})\varphi_i(\hat{r}) \right) d\hat{r} \quad (43)$$

$$F_i = \int_0^1 \left( \frac{\hat{V}^{\,i}\delta\hat{V}}{(1-\hat{w}_s)^2}\varphi_i(\hat{r}) \right) d\hat{r} \quad (44)$$

By solving above mentioned equations, the deflection of the diaphragm can be determined at applied electrostatic force.

**3. 2. Dynamic Analysis** For studying the dynamic response of the microplate, a Galerkin based reduced order model can be used [37]. Due to the nonlinear term in Equation (33), direct use of the Galerkin method is not applicable so it assumed as a forcing term and integration over this term is repeated at each time step [38]. Considering small enough time steps leads to a proper convergence result.

The approximated solution for solving the dynamic equation of the diaphragm deflection is defined as:

$$\hat{w}_d(\hat{r},\hat{t}) = \sum_{n=1}^{N} q_n(\hat{t})\varphi_n(\hat{r}) \quad (45)$$

In which $q_n(\hat{t})$ are the generalized coordinates and $\varphi_n(\hat{r})$ are shape functions satisfied all boundary conditions of clamped circular diaphragm. By substituting Equation (45) into Equation (33) and multiplying the weight function $\varphi_i(\hat{r})$ in the Galerkin method, and integrating the outcome over $\hat{r}=[0\ 1]$ a Galerkin-based reduced order model is generated as:

$$\sum_{n=1}^{N}\left(M_{in}\ddot{q}_n + C_{in}\dot{q}_n + K_{in}q_n\right) = F_i\left(\hat{w}_s,\hat{t}\right) \quad \text{i=1,2,...N} \quad (46)$$

where, M, C, K are mass, damping and stiffness matrices, respectively and F determines the forcing vector. All the mentioned elements are calculated as follows:

$$M_{in} = \int_0^1 \varphi_i(\hat{r})\varphi_n(\hat{r})d\hat{r} \quad (47)$$

$$C_{in} = \beta\int_0^1 \varphi_i(\hat{r})\varphi_n(\hat{r})d\hat{r} \quad (48)$$

$$K_{in} = \int_0^1 \varphi_i(\hat{r})\left( (\frac{D+D^{\ell}}{D})\nabla^4 \varphi_n(\hat{r}) \right) d\hat{r} \quad (49)$$

$$F_i = \int_0^1 \left( \varphi_i(\hat{r})\frac{\hat{V}^{\,2}}{2(1-\hat{w}\ )^2} \right) d\hat{r} \quad (50)$$

By solving above mentioned equations, the response of the circular diaphragm can be determined at any time.

**3. 3. Volumetric Flow Rate Formulation** Recognizing the mechanical behavior of the micropump provides this opportunity to investigate the volumetric

flow rate of the micropump with the circular diaphragm. Volumetric flow is a function of the excitation frequency and the amplitude and can be calculated as follows:

$$Q = \forall \times \hat{f} \tag{51}$$

$$\forall = \int_0^1 2\pi \hat{r}.\hat{w}\,(\hat{r},\hat{t})_{\max}\, d\hat{r} \tag{52}$$

Considering that $\hat{\omega} = 2\pi\hat{f}$ and $\hat{w}(\hat{r},\hat{t})_{\max} = a\varphi(\hat{r})$ and substituting Equation (52) into Equation (51) the volumetric flow rate can be calculated as:

$$Q = \int_0^1 a\varphi(\hat{r}).\hat{\omega}.\hat{r}\; d\hat{r} \tag{53}$$

where, $\forall$ is the volume, Q is the volumetric flow and $\hat{f}$ and $\hat{\omega}$ are the ordinary and angular frequencies.

## 4. NUMERICAL RESULTS AND DISCUSSION

With the purpose of studying the mechanical behavior of a micropump with a circular clamped diaphragm actuated by electrostatic force the geometrical and material properties of the microstructure is listed in Tables 1 and 2 respectively.

The following axisymmetric shape function which satisfies all boundary conditions for the circular microplate is utilized:

$$\varphi(\hat{r}) = (\hat{r}-1)^2(\hat{r}+1)^2 \tag{54}$$

**TABLE 1.** Geometrical properties of the diaphragm

| Parameters | Values |
|---|---|
| Radius (R) | 230 µm |
| Thickness (h) | 2.25 µm |
| Permittivity of air( $\varepsilon_0$ ) | $8.8541878\times10^{-12}$ F m$^{-1}$ |
| Initial gap ($g_0$) | 2 µm |

**TABLE 2.** Material properties of the diaphragm

| Parameters | Values |
|---|---|
| Young's modulus (E) | 169 GPa |
| Poisson's ratio ( $\nu$ ) | 0.22 |
| Density ( $\rho$ ) | 2330 kg m$^{-3}$ |

In this article, for evaluating the effect of length scale parameter, length scale ratio ($\ell_r$) is introduced which is the ratio of length scale parameter ($\ell$) to the microplate thickness (h):

$$\ell_r = \frac{\ell}{h} \tag{55}$$

**4. 1. Static Response of the Diaphragm to Bias DC Voltage** In order to study the static behavior of the diaphragm, different bias DC voltages are applied. As the voltage increases the equivalent stiffness of the microplate decreases and the diaphragm is more deflected toward the ground plate until it causes the displacement to reach a point that no stable equilibrium exists and the diaphragm collapses on the ground plate. This voltage is called static pull-in voltage which limits the applied voltage.

Figure 2 depicts the non-dimensional center deflection of the clamped microplate versus different non-dimensional bias voltages using modified couple stress theory for different length scale ratios. According to the diagram, the predicted static pull-in voltage based on MCST in all different length scale ratios is higher than CT under the same conditions. In addition, as the length scale ratio increases, the static pull-in voltage reaches higher values which means that static pull-in voltage of the micro structures is dramatically size dependent. The obtained results based on CT have a good agreement with those reported in literature [3].

**4. 2. Dynamic Response of the Diaphragm to Step DC Voltage** In order to study the dynamic behavior of the diaphragm a step DC voltage is applied to the microplate. There is a limitation on the threshold of the step DC voltage which is applied to the micropump on account of dependency of the displacement to the electrostatic force. The value of this voltage is known as dynamic pull-in voltage which is as low as 90-92% of static pull-in voltage [39].

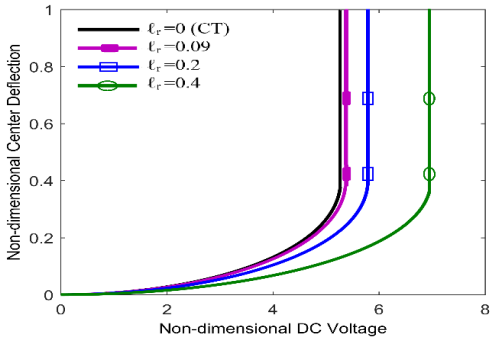


**Figure 2.** Static pull-in variation for different length scale ratios based on modified couple stress theory in comparison to classical theory

The equation of the dynamic motion is converted to a reduced order model and by applying fourth-order Runge-Kutta method, the results can be integrated over time. Figures 3 and 4 depict the phase portrait and time history diagrams of the non-dimensional center deflection of the diaphragm using modified couple stress theory for different length scale ratios, respectively. Continious mode of time history diagram in Figure 4, turns into unstable mode in Figure 5 by low voltage rising which is known as dynamic pull-in instibility. Similar to static pull-in voltage, as the length scale ratio increases, according to Figure 5, the dynamic pull-in voltage reaches higher values and as shown in the figure, the dynamic pull-in voltage is as low as 90-92% of the static pull-in voltage due to the inertial forces.

**4. 3. Frequency Response of the Diaphragm** Figure 6 illustrates the frequency response of the micropump for different length scale ratios based on modified couple stress theory. It is clear that the maximum deflection in all states occurs when the frequency is equal to its natural frequency of the system. In addition, it is deduced that under the same bias voltage, as the length scale ratio arises, the natural frequency increases and the central deflection decreases. This is caused by increment of the system stiffness using MCST. In other words, CT predicts more deflection and less natural frequency than MCST.

The bias voltage effect on the frequency response of the micropump for $\ell_r$=0.2 in different applied bias DC voltages is shown in Figure 7. According to the diagram it is inferred that by increasing the bias voltage value, the natural frequency decreases but the deflection reaches higher values. This is because of the system stiffness reduction due to the applying higher values of the bias voltage.

**4. 4. Volumetric Flow Rate** Figure 8 depicts the volumetric flow rate using modified couple stress theory in various length scale ratios. According to the diagram maximum flow rate for each state occurs in natural frequency of the system.

Furthermore, in the same bias voltage, increment of the length scale ratio reduces volumetric flow rate since applying MCST causes the system to be stiffer. In other

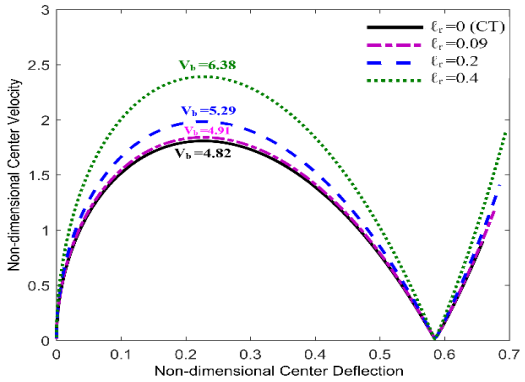


**Figure 3.** Phase portraits of the clamped microplate for different length scale ratios based on modified couple stress theory in comparison to classical theory

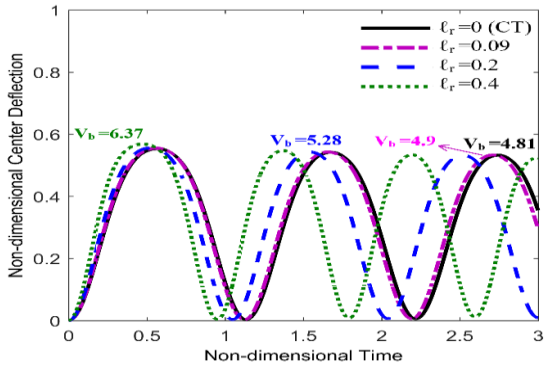


**Figure 4.** Time history of the diaphragm due to application of a step DC voltage based on modified couple stress theory for different length scale ratios in comparison to classical theory

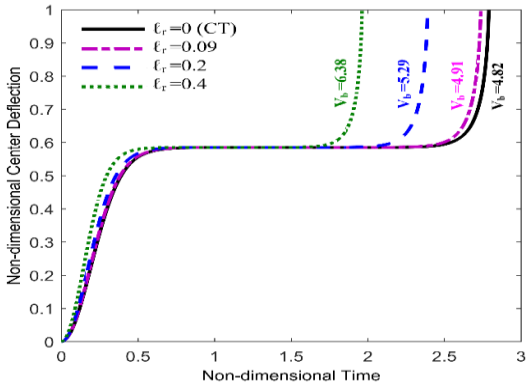


**Figure 5.** Dynamic pull-in variation for different length scale ratios based on modified couple stress theory in comparison to classical theory

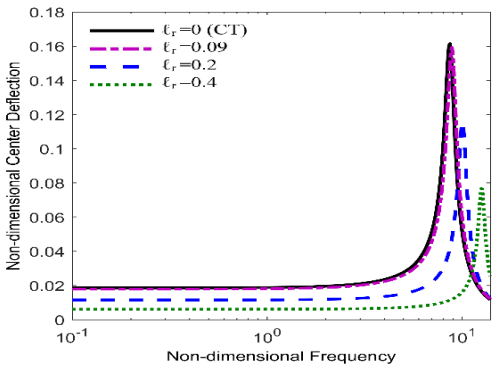


**Figure 6.** Frequency response of the diaphragm for different length scale ratios based on modified couple stress theory in comparison to classical theory

words, CT predicts more flow rate and less natural frequency than MCST. The bias voltage effect on flow rate of the micropump using modified couple stress theory for $\ell_r$=0.2 in different applied bias DC voltages is shown in Figure 9.

It is deduced that in higher range of voltage the flow rate is higher and the natural frequency is lower owing to the system stiffness reduction due to the applying higher values of bias voltage.

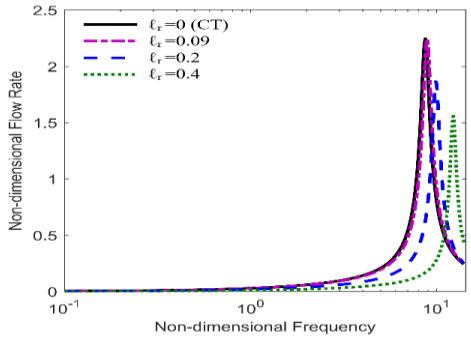


**Figure 7.** Frequency response of the diaphragm for $\ell_r$=0.2 based on modified couple stress theory in different bias DC voltages

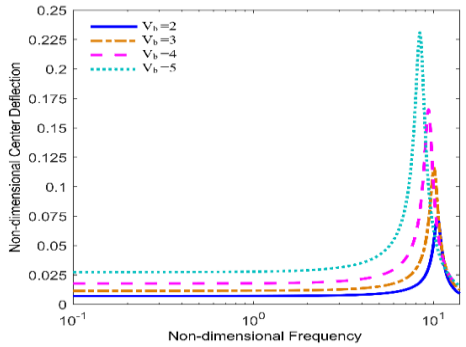


**Figure 8.** Volumetric flow rate of the micropump using modified couple stress theory in various length scale ratios in comparison to classical theory

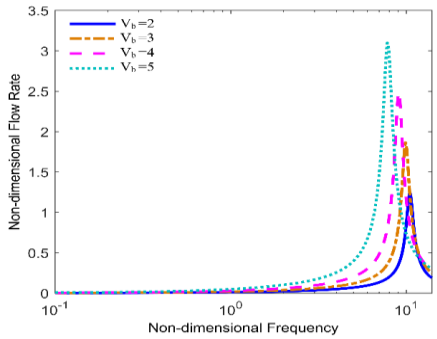


**Figure 9.** Bias voltage effect on volumetric flow rate of the micropump using modified couple stress theory for $\ell_r$=0.2 in different bias DC voltages

## 5. CONCLUSIONS

This paper studied the size dependent behavior of a micropump with circular diaphragm using MCST. The numerical results showed that both static and dynamic pull-in voltages calculated by modified couple stress theory was more than that calculated by the classical ones. As the length-scale ratio was increased the pull-in voltage raised. According to the results, for $\ell_r$=0.2, the value of pull-in voltage rise is 9.84% in static analysis and 9.75% in dynamic analysis.The stiffness of the microplate increased under MCST and as a result of that in a particular bias voltage, as the length scale ratio increased, the central deflection decreased. According to the results for $\ell_r$=0.2, decrement of deflection is 28.12% under the same excitation voltage and the results showed that bias voltage increment caused more deflection and less natural frequency.The results expressed that maximum volumetric flow rate occurred in natural frequency of the system. Furthermore, increment of length scale ratio reduced the volumetric flow rate and for $\ell_r$=0.2, decrement of volumetric flow rate is 16.66% and the results showed that in higher range of bias voltage the flow rate was higher and the natural frequency was lower.

This paper has proved that the mechanical behaviour of the micropump should be studied under modified couple stress theory since the classical theory may lead to inaccurate results in studying the mechanical behaviour of the diaphragm with considerable material length scale parameter. This becomes a big deal especially in small scales.

## 6. REFERENCES

1. Rashvand, K., Rezazadeh, G. and Madinei, H., "Effect of length-scale parameter on pull-in voltage and natural frequency of a micro-plate", ***International Journal of Engineering***, Vol. 27, No. 3, (2014), 375-384.
2. Liu, J., Martin, D.T., Kadirvel, K., Nishida, T., Cattafesta, L., Sheplak, M. and Mann, B.P., "Nonlinear model and system identification of a capacitive dual-backplate mems microphone", ***Journal of Sound and Vibration***, Vol. 309, No. 1-2, (2008), 276-292.
3. Saeedivahdat, A., Abdolkarimzadeh, F., Feyzi, A., Rezazadeh, G. and Tarverdilo, S., "Effect of thermal stresses on stability and frequency response of a capacitive microphone", ***Microelectronics Journal***, Vol. 41, No. 12, (2010), 865-873.
4. Zhou, Z., Wang, Z. and Lin, L., "Microsystems and nanotechnology, Springer, (2012).
5. Bhat, K., Nayak, M., Kumar, V., Thomas, L., Manish, S., Thyagarajan, V., Gaurav, S., Bhat, N. and Pratap, R., Design, development, fabrication, packaging, and testing of mems pressure sensors for aerospace applications, in Micro and smart devices and systems. 2014, Springer.3-17.
6. Lemarquand, G., Ravaud, R., Shahosseini, I., Lemarquand, V., Moulin, J. and Lefeuvre, E., "Mems electrodynamic loudspeakers for mobile phones", ***Applied Acoustics***, Vol. 73, No. 4, (2012), 379-385.

7. Ferrari, M., "Biomems and biomedical nanotechnology: Volume ii: Micro/nano technologies for genomics and proteomics, Springer Science & Business Media, Vol. 2, (2007).
8. Ashraf, M.W., Tayyaba, S. and Afzulpurkar, N., "Micro electromechanical systems (mems) based microfluidic devices for biomedical applications", ***International journal of molecular sciences***, Vol. 12, No. 6, (2011), 3648-3704.
9. Nisar, A., Afzulpurkar, N., Mahaisavariya, B. and Tuantranont, A., "Mems-based micropumps in drug delivery and biomedical applications", ***Sensors and Actuators B: Chemical***, Vol. 130, No. 2, (2008), 917-942.
10. Sen, M., Wajerski, D. and Gad-el-Hak, M., "A novel pump for mems applications", ***Journal of Fluids Engineering, Transactions of the ASME***, Vol. 118, No. 3, (1996), 624-627.
11. Judy, J.W., Tamagawa, T. and Polla, D.L., "Surface-machined micromechanical membrane pump", in Micro Electro Mechanical Systems, 1991, MEMS'91, Proceedings. An Investigation of Micro Structures, Sensors, Actuators, Machines and Robots. IEEE, IEEE., (1991), 182-186.
12. Zengerle, R., Richter, A. and Sandmaier, H., "A micro membrane pump with electrostatic actuation", in Micro Electro Mechanical Systems, 1992, MEMS'92, Proceedings. An Investigation of Micro Structures, Sensors, Actuators, Machines and Robot. IEEE, IEEE., (1992), 19-24.
13. Machauf, A., Nemirovsky, Y. and Dinnar, U., "A membrane micropump electrostatically actuated across the working fluid", ***Journal of Micromechanics and Microengineering***, Vol. 15, No. 12, (2005), 2309.
14. Liu, W.-y., "Research on electrostatic micropump pull-in phenomena based on reduced order model", in Intelligent Computation Technology and Automation (ICICTA), 2010 International Conference on, IEEE. Vol. 2, (2010), 1154-1157.
15. Li, L., Zhu, R., Zhou, Z. and Ren, J., "Modeling of a micropump membrane with electrostatic actuator", in Advanced Computer Control (ICACC), 2010 2nd International Conference on, IEEE. Vol. 5, (2010), 630-632.
16. Zhao, Y.-P., Wang, L. and Yu, T., "Mechanics of adhesion in mems—a review", ***Journal of Adhesion Science and Technology***, Vol. 17, No. 4, (2003), 519-546.
17. Nabian, A., Rezazadeh, G., Haddad-Derafshi, M. and Tahmasebi, A., "Mechanical behavior of a circular micro plate subjected to uniform hydrostatic and non-uniform electrostatic pressure", ***Microsystem Technologies***, Vol. 14, No. 2, (2008), 235-240.
18. Zhang, Y. and Zhao, Y.-p., "Numerical and analytical study on the pull-in instability of micro-structure under electrostatic loading", ***Sensors and Actuators A: Physical***, Vol. 127, No. 2, (2006), 366-380.
19. Mobki, H., Sadeghia, M. and Rezazadehb, G., "Design of direct exponential observers for fault detection of nonlinear mems tunable capacitor", ***IJE Transactions A: Basics***, Vol. 28, No. 4, (2015), 634-641.
20. Dowlati, S., Rezazadeh, G., Afrang, S., Sheykhlou, M. and Pasandi, A.M., "An accurate study on capacitive microphone with circular diaphragm using a higher order elasticity theory", ***Latin American Journal of Solids and Structures***, Vol. 13, No. 4, (2016), 590-609.
21. Khanchehgardan, A., SHAH, M.A.A., Rezazadeh, G. and Shabani, R., "Thermo-elastic damping in nano-beam resonators based on nonlocal theory", Vol. 26, No. 12, (2013), 1505-1514.
22. SHAH, M.A.A., Khanchehgardan, A., Rezazadeh, G. and Shabani, R., "Mechanical response of a piezoelectrically sandwiched nano-beam based on the nonlocal theory", Vol. 26, No. 12, (2013), 1515-1524.
23. Loh, O.Y. and Espinosa, H.D., "Nanoelectromechanical contact switches", ***Nature Nanotechnology***, Vol. 7, No. 5, (2012), 283.
24. Sadeghian, H., Yang, C.-K., Goosen, J.F., Bossche, A., Staufer, U., French, P.J. and van Keulen, F., "Effects of size and defects on the elasticity of silicon nanocantilevers", ***Journal of Micromechanics and Microengineering***, Vol. 20, No. 6, (2010) doi: 10.1088/0960-1317/20/6/064012.
25. Abazari, A.M., Safavi, S.M., Rezazadeh, G. and Villanueva, L.G., "Modelling the size effects on the mechanical properties of micro/nano structures", ***Sensors***, Vol. 15, No. 11, (2015), 28543-28562.
26. Tsiatas, G.C., "A new kirchhoff plate model based on a modified couple stress theory", ***International Journal of Solids and Structures***, Vol. 46, No. 13, (2009), 2757-2764.
27. Lazopoulos, K., "On bending of strain gradient elastic micro-plates", ***Mechanics Research Communications***, Vol. 36, No. 7, (2009), 777-783.
28. Eringen, A.C., "On differential equations of nonlocal elasticity and solutions of screw dislocation and surface waves", ***Journal of Applied Physics***, Vol. 54, No. 9, (1983), 4703-4710.
29. Reddy, J., "Nonlocal nonlinear formulations for bending of classical and shear deformation theories of beams and plates", ***International Journal of Engineering Science***, Vol. 48, No. 11, (2010), 1507-1518.
30. Toupin, R.A., "Elastic materials with couple-stresses", ***Archive for Rational Mechanics and Analysis***, Vol. 11, No. 1, (1962), 385-414.
31. Cosserat, E. and Cosserat, F., "Théorie des corps déformables", Vol., No., (1909).
32. Mindlin, R. and Tiersten, H., "Effects of couple-stresses in linear elasticity", ***Archive for Rational Mechanics and Analysis***, Vol. 11, No. 1, (1962), 415-448.
33. Yang, F., Chong, A., Lam, D.C.C. and Tong, P., "Couple stress based strain gradient theory for elasticity", ***International Journal of Solids and Structures***, Vol. 39, No. 10, (2002), 2731-2743.
34. Jomehzadeh, E., Noori, H. and Saidi, A., "The size-dependent vibration analysis of micro-plates based on a modified couple stress theory", ***Physica E: Low-dimensional Systems and Nanostructures***, Vol. 43, No. 4, (2011), 877-883.
35. Timoshenko, S.P. and Woinowsky-Krieger, S., "Theory of plates and shells, McGraw-Hill, (1959).
36. Leech, C., "Beam theories: A variational approach", ***International Journal of Mechanical Engineering Education.***, Vol. 5, (1977), 81-87.
37. Vogl, G.W. and Nayfeh, A.H., "A reduced-order model for electrically actuated clamped circular plates", ***Journal of Micromechanics and Microengineering***, Vol. 15, No. 4, (2005), 684.
38. Sharafkhani, N., Rezazadeh, G. and Shabani, R., "Study of mechanical behavior of circular fgm micro-plates under nonlinear electrostatic and mechanical shock loadings", ***Acta Mechanica***, Vol. 223, No. 3, (2012), 579-591.
39. Nayfeh, A.H., Younis, M.I. and Abdel-Rahman, E.M., "Dynamic pull-in phenomenon in mems resonators", ***Nonlinear Dynamics***, Vol. 48, No. 1-2, (2007), 153-163.

# Study of Volumetric Flow Rate of a Micropump Using a Non-Classical Elasticity Theory

A. M. Pasandi[a], S. Afrang[a], S. Dowlati[a], N. Sharafkhani[b], G. Rezazadeh[c]

[a] *Electrical Engineering Department, Urmia University, Urmia, Iran*
[b] *Mechanical Engineering Department, Tabriz University, Tabriz, Iran*
[c] *Mechanical Engineering Department, Urmia University, Urmia, Iran*

*P A P E R I N F O*

*Paper history:*
Received 11 May 2016
Received in revised form 08 November 2017
Accepted 02 December 2017

*Keywords*:
*MEMS*
*Micropump*
*Pull-in phenomenon*
*Couple Stress Theory*

**چکیده**

هدف از این تحقیق مطالعه رفتار مکانیکی یک میکروپمپ با دیافراگم دایره ای چسبیده است که جز اصلی سیستمهای تحویل دارو است. در این مقاله معادلات غیرخطی حاکم بر میکروپلیت دایره ای با استفاده از تئوری صفحات نازک کیرشهف، بر اساس فشار دوگانه اصلاح شده (MCST) و تئوریهای کلاسیک (CT) استخراج شده است.سپس معادله غیرخطی انحراف استاتیک با استفاده از روش خطی گام به گام (SSLM) حل می‌شود تا از غیرخطی بودن معادله دیفرانسیل بگریزیم و مدل کاهش مرتبه بر مبنای روش گالرکین برای بررسی حرکت پویای میکروپلیت مورد استفاده قرار می گیرد. پس از آن ثبات استاتیکی و دینامیکی میکروپمپ بر اساس MCST و CT مورد بررسی قرار گرفت و سپس مقایسه شد.همچنین میزان جریان حجمی میکروپمپ بر اساس تئوریها و کل پژوهش بررسی شده است. حضور پارامتر مقیاس طول در نظریه فشار دوگانه اصلاح شده این فرصت رابوجود می آورد که اثر اندازه بر رفتار مکانیکی میکروپمپ را بررسی کنیم.

***doi**: 10.5829/ije.2018.31.06c.17*